Effect of Cavity Size on the Charge Distribution in Carbido-Metal Carbonyl Clusters and Its Possible Catalytic Implications

Jean-Francois Halet,† David G. Evans,‡ and D. Michael P. Mingos*†

Contribution from the Inorganic Chemistry Laboratory, University of Oxford, South Parks Road, Oxford OX1 3QR, United Kingdom, and Department of Chemistry, University of Exeter, Exeter EX4 4QD, United Kingdom. *Received April 30, 1987*

Abstract: Molecular orbital calculations on carbido-transition-metal carbonyl cluster compounds where the carbon atom lies in a large cavity indicate a substantial buildup of negative charge on the carbon atom. Besides making the carbon more susceptible to protonic attack the large cavity assists the stabilization of interstitial C-H fragments.

The importance of carbido cluster compounds as models for intermediates in Fischer-Tropsch catalytic processes is well-recognized and has stimulated several theoretical analyses.[1,2] The carbido ligand has now been stabilized in different polyhedral cavities and coordination environments (see Table I, for example). Theoretical studies have focussed particularly on those carbido clusters where the carbon atom occupies an exposed site,[1] e.g., butterfly $[Fe_4(CO)_{12}(\mu_4\text{-}C)]^{2-}$ and square pyramidal $[Fe_5(CO)_{15}(\mu_5\text{-}C)]$. The greater reactivity of the former has been related to these asymmetry effects.[8] The discovery of carbido ligands in larger square-antiprismatic cavities in both molecular,[9] e.g., $[Ni_8(CO)_{16}(\mu_8\text{-}C)]^{2-}$, and infinite solids,[10] e.g., $Cr_{23}C_6$, prompted us to study the effect of cavity size on the metal-carbon bonding and the charge on the carbon atom. The results have proved to be particularly interesting, because they have suggested that a carbon atom within a large cavity bears a substantial negative charge and should be very susceptible to electrophilic reagents.[11] The results of the molecular orbital calculations on model carbido clusters with 4-12 metal atoms are summarized in Table II. Geometrically this change in metal nuclearity corresponds to a substantial increase in metal-carbon distance from 1.80 Å (octahedron) to 2.42 Å (icosahedron), if a metal-metal distance of 2.54 Å is taken as representative for a cobalt-cobalt bond.

Bonding of the Carbon Atom in Small Cavities

In the octahedral cluster $[Co_6L_{18}(\mu_6\text{-}C)]^{8+}$ (**3**), with D_{3d} symmetry, the metal-carbon bonding[2] occurs primarily through the carbon 2s and 2p orbitals and the cluster S^{σ} and $P^{\pi/\sigma}$ skeletal molecular orbitals (labeled according to the Tensor Surface Harmonic Theory[12]) shown on the left-hand side of Figure 1. The delocalized nature of the bonding leads to a carbon that is nearly electroneutral and a metal-carbon overlap population of 0.42. The metal contribution to this bonding arises primarily from the $P^{\pi/\sigma}$ tangential skeletal molecular orbitals derived from the ML_3 e frontier hybrid orbitals.[13] The antibonding components of this interaction are outside the frontier orbital region and their antibonding character is only mitigated by mixing with the higher lying $P^{\sigma/\pi}$ skeletal molecular orbitals derived from the ML_3 a_1 radial orbitals. This mixing is illustrated in **11** for the $P^{\sigma/\pi}_{1c}$ component (only the metallic sp contributions are shown for clarity).

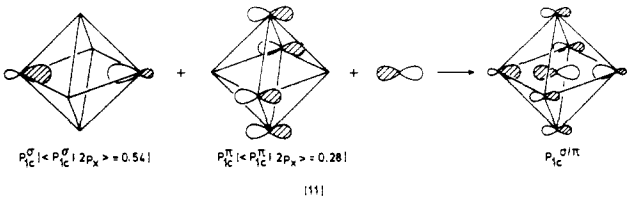

[11]

† University of Oxford.
‡ University of Exeter.

Table I. Observed Environment of the Carbon Atom in Carbido-Transition-Metal Carbonyl Cluster Compounds

cage	example	VEC[a]	$d_{M\text{-}C}$ (Å)	$d_{M\text{-}M}$ (Å)	ref
butterfly	$(Fe_4(CO)_{12}(\mu_4\text{-}C)]^{2-}$	62	1.80/1.99	2.62	3
square pyramid	$Fe_5(CO)_{15}(\mu_5\text{-}C)$	74	1.90	2.64	4
octahedron	$[Co_6(CO)_{13}(\mu_6\text{-}C)]^{2-}$	86	1.87	2.47/2.93	5
trigonal prism	$[Co_6(CO)_{15}(\mu_6\text{-}C)]^{2-}$	90	1.95	2.55	6
square antiprism	$[Ni_8(CO)_{16}(\mu_8\text{-}C)]^{2-}$	118	2.08	2.48/2.63	7

[a] Valence electron count.

An indication of the effect of placing the carbon atom in an asymmetric environment is afforded by the calculation on $[Co_5(CO)_{15}(\mu_5\text{-}C)]^{5+}$ (**2**), where the carbon atom lies 0.15 Å below the base of the square pyramid.[1b,e] The computed charge of -0.10 indicates that the effect is not large. For the butterfly $[Fe_4(CO)_{12}(\mu_4\text{-}C)]^{2-}$ cluster a computed charge of -0.60 has been reported with use of Fenske-Hall calculations.[1c] These Extended Hückel calculations give a charge of -0.27 for the cluster model $[Co_4(CO)_{12}(\mu_4\text{-}C]^{2+}$ (**1**) (see Table II). Both results are consistent

(1) (a) Kolis, J. W.; Basolo, F.; Shriver, D. F. *J. Am. Chem. Soc.* **1982**, *104*, 5626. (b) Wijeyesekara, S. D.; Hoffmann, R.; Wilker, C. N. *Organometallics* **1984**, *3*, 962. (c) Harris, S.; Bradley, J. S. *Organometallics* **1984**, *3*, 1086. (d) Housecroft, C. E. *J. Organomet. Chem.* **1984**, *276*, 297. (e) Halet, J.-F.; Saillard, J.-Y.; Lissillour, R.; McGlinchey, M. J.; Jaouen, G. *Organometallics* **1986**, *5*, 139. (f) Brint, P.; O'Cuill, K.; Spalding, T. R. *Polyhedron* **1986**, *5*, 1791. (g) Chisholm, M. H.; Clark, D. L.; Huffman, J. C.; Smith, C. A. *Organometallics*, in press.
(2) Wijeyesekara, S. D.; Hoffmann, R. *Organometallics* **1984**, *3*, 949.
(3) Boehme, R. F.; Coppens, P. *Acta Crystallogr.* **1981**, *B37*, 1914.
(4) Braye, E. H.; Dahl, L. F.; Hübel, W.; Wampler, D. L. *J. Am. Chem. Soc.* **1962**, *84*, 4633.
(5) Albano, V. G.; Braga, D.; Martinengo, S. *J. Chem. Soc., Dalton Trans.* **1986**, 981.
(6) Martinengo, S.; Strumolo, D.; Chini, P.; Albano, V. G.; Braga, D. *J. Chem. Soc., Dalton Trans.* **1985**, 35.
(7) Ceriotti, A.; Longoni, G.; Manassero, M.; Perego, M.; Sansoni, M. *Inorg. Chem.* **1985**, *24*, 117.
(8) See, for example: Bradley, J. S. *Adv. Organomet. Chem.* **1983**, *22*, 1 and references therein.
(9) (a) Albano, V. G.; Chini, P.; Ciani, G.; Martinengo, S.; Sansoni, M. *J. Chem. Soc., Dalton Trans.* **1978**, 463. (b) Longoni, G.; Ceriotti, A.; Della Pergola, R.; Manassero, M.; Sansoni, M. *J. Chem. Soc., Dalton Trans.* **1984**, 1181. (c) Ceriotti, A.; Longoni, G.; Manassero, M.; Perego, M.; Sansoni, M. *Inorg. Chem.* **1985**, *24*, 117. (d) Ceriotti, A.; Longoni, G.; Piro, G.; Resconi, L.; Demartin, F.; Manassero, M.; Masciocchi, N.; Sansoni, M. *J. am. Chem. Soc.* **1986**, *108*, 8091.
(10) Bowman, A. L.; Arnold, G. P.; Storms, E. K.; Nereson, N. G. *Acta Crystallogr.* **1972**, *B28*, 3102.
(11) Longoni, G.; Ceriotti, A.; Marchionna, M.; Piro, G., to be published.
(12) For an introduction on the Tensor Surface Harmonic Theory see: (a) Stone, A. J. *J. Mol. Phys.* **1980**, *41*, 1339. (b) Stone, A. J. *Inorg. Chem.* **1981**, *20*, 563. (c) Stone, A. J.; Alderton, M. J. *Inorg. Chem.* **1982**, *21*, 2297. (d) Stone, A. J. *Polyhedron* **1984**, *3*, 3051. (e) Mingos, D. M. P.; Hawes, J. C. *Struct. Bond.* **1985**, *63*, 1. (f) Mingos, D. M. P. *Pure Appl. Chem.* **1987**, *59*, 145.
(13) Albright, T. A.; Hoffman, P.; Hoffmann, R. *J. Am. Chem. Soc.* **1977**, *99*, 7546.

0002-7863/88/1510-0087$01.50/0

Table II. Computed Results on the Different Carbido Cluster Models

model	geometry	VEC[a]	d_{M-C} (Å)	carbon orbital occupation				pop.	carbon charge
				$2p_z$	$2p_y$	$2p_x$	2s		
$[Co_4(CO)_{12}(\mu_4\text{-}C)]^{2+}$ (**1**)	butterfly (C_{2v})	62	1.80	0.99	0.87	0.86	1.54	0.65/0.48	−0.27
$[Co_5(CO)_{15}(\mu_5\text{-}C)]^{5+}$ (**2**)	square pyramid ("C_{4v}")	74	1.8/1.95	0.80	0.81	0.81	1.52	0.52/0.29	−0.10
$[Co_5L_{15}(\mu_5\text{-}C)]^{5+}$ (**2'**)	square pyramid ("C_{4v}")	74	1.8/1.95	0.80	0.87	0.87	1.53	0.51/0.30	−0.06
$[Co_6L_{18}(\mu_6\text{-}C)]^{8+}$ (**3**)	octahedron (D_{3d})	86	1.80	0.80	0.81	0.81	1.49	0.42	0.09
$[Co_6L_{18}(\mu_6\text{-}C)]^{4+}$ (**4**)	trigonal prism (D_{3h})	90	1.94	0.84	0.85	0.85	1.54	0.39	−0.09
$[Co_8(\mu\text{-}L)_8L_8(\mu_8\text{-}C)]^{6-}$ (**5**)	square antiprism (D_{4d})	114	2.09	0.79	0.84	0.84	1.58	0.26	−0.05
$[Co_8(\mu\text{-}L)_8L_8(\mu_8\text{-}C)]^{10-}$ (**6**)	square antiprism (D_{4d})	118	2.09	0.80	1.36	1.36	1.58	0.28	−1.09
$[Co_{10}(\mu_3\text{-}L)_8L_{10}(\mu_8\text{-}C)]^{4-}$ (**7**)	bicapped square antiprism (D_{4d})	142	2.09	0.78	1.34	1.34	1.58	0.28	−1.04
			2.86					−0.02	
$[Co_{12}(\mu_3\text{-}L)_{10}L_{12}(\mu_{12}\text{-}C)]^{14-}$ (**8**)	icosahedron (D_{5d})	170	2.42	0.81	1.46	1.46	1.60	0.15	−1.42
								0.08	
$[Co_8(\mu\text{-}L)_8L_8(\mu_8\text{-}P)]^{9-}$ (**9**)	square antiprism (D_{4d})	118	2.09[b]	1.01[b]	1.28[b]	1.28[b]	1.43[b]	0.39[b]	0.00[b]
$[Co_{10}(\mu_3\text{-}L)_8L_{10}(\mu_8\text{-}Si)]^{4-}$ (**10**)	bicapped square antiprism (D_{4d})	142	2.09[b]	0.46	0.95[b]	0.95[b]	1.32[b]	0.40[b]	0.31[b]
			2.86					−0.04	

[a] Valence electron count. [b] Corresponding values for the P and Si interstitial atoms.

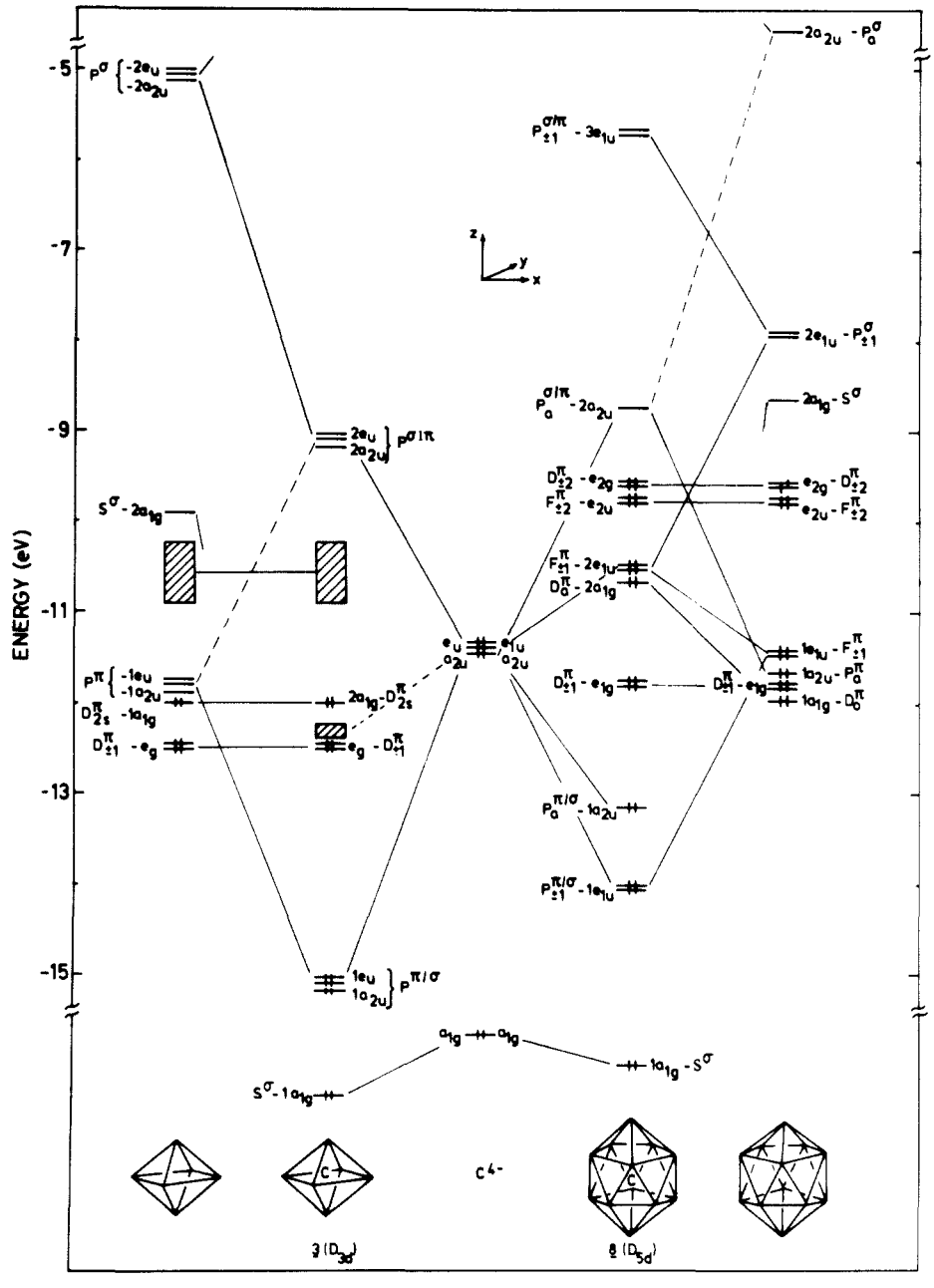

Figure 1. Molecular orbital interaction diagram for $[Co_6L_{18}(\mu_6\text{-}C)]^{8+}$ (**3**) with D_{3d} symmetry (left-hand side) and for $[Co_{12}(\mu_3\text{-}L)_{10}L_{12}(\mu_{12}\text{-}C)]^{14-}$ (**8**) with D_{5d} symmetry (right-hand side). The hatched areas on the left-hand side correspond either to d-band molecular orbitals or metal–ligand molecular orbitals.

with the nucleophilic nature of the exposed carbon atom in butterfly carbido cluster compounds.[8]

Bonding of the Carbon Atom in Large Cavities

The results for icosahedral $[Co_{12}(\mu_3\text{-}L)_{10}L_{12}(\mu_{12}\text{-}C)]^{4-}$ (**8**) with D_{5d} symmetry are illustrated on the right-hand side of Figure 1. The weaker metal–carbon interactions are reflected directly in the smaller metal–carbon overlap populations (0.15 to equatorial and 0.08 to axial metal atoms) and indirectly in a much more negatively charged carbon atom (−1.42). From Table II it is

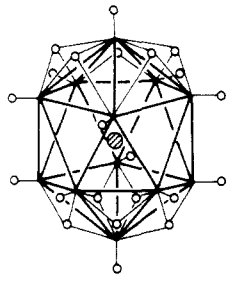

(8)

apparent that the latter arises from substantially more electron density in the carbon $2p_x$ and $2p_y$ orbitals resulting from the population of the metal–carbon nonbonding $F^{\pi}_{\pm 1}(2e_{1u})$ molecular orbital in Figure 1. In the larger cavity the carbon 2p orbitals interact more weakly with the cluster tangential molecular orbitals ($F^{\pi}_{\pm 1}(e_{1u})$ and $P^{\pi}_{0}(a_{2u})$ in **8**), and consequently the antibonding component of this interaction is low-lying. Furthermore, the radial $P^{\sigma/\pi}_{\pm 1}$ cluster molecular orbitals are lower lying and mix more extensively with these antibonding components (see **12** for the metal–carbon nonbonding F^{π}_{1c} component). This stabilization of the e_{1u} components is sufficient for them to enter into the expanded

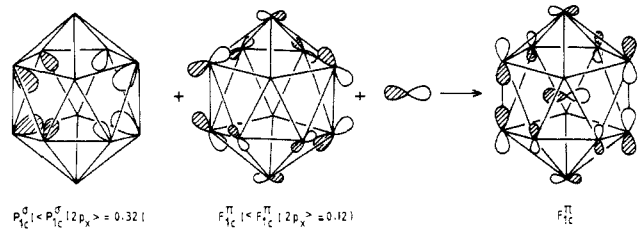

band of skeletal molecular orbitals. Furthermore the extensive $P^{\sigma}_{\pm 1} - F^{\pi}_{\pm 1}$ mixing ensures that these orbitals are not strongly metal–carbon antibonding. The actual anisotropic C charge distribution is due to the lowering of symmetry of **8** from I_h to D_{5d}. The triply bridging ligands emulate a P^{σ}_{0} orbital which interacts with the metallic P^{σ}_{0} level and pushes it out of the bonding region. Thus the M–C nonbonding $P^{\sigma/\pi}_{0}$ molecular orbital is vacant and is the LUMO of **8**. This means that the arrangement of the ligand shell may induce a substantial asymmetry in the metal–interstitial carbon bonding.[14]

The calculations on clusters with intermediate nuclearities suggest that the buildup of charge on the carbido atom is not a linear process, but it occurs abruptly when the M–C nonbonding $L^{\pi}_{\pm 1}$ components enter into the skeletal bonding region. In our model calculations this crossover occurs for square-antiprismatic cavities. For the square antiprism, two-electron counts associated with closo and arachno structural designations are possible and are observed in $[Co_8(CO)_{18}(\mu_8\text{-}C)]^{2-}$ (114 valence electrons, distorted square antiprism)[9a,15] and $[Ni_8(CO)_{16}(\mu_8\text{-}C)]^{2-}$ (118 valence electrons, regular square antiprism).[7] The calculations on the model compounds $[Co_8(\mu\text{-}L)_8L_8(\mu_8\text{-}C)]^{6-}$ (**5**) with 114 electrons and $[Co_8(\mu\text{-}L)_8L_8(\mu\text{-}C)]^{10-}$ (**6**) with 118 electrons suggest that the additional four electrons occupy the M–C nonbonding

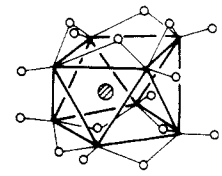

(5) (6)

$D^{\pi}_{\pm 1}(e_1)$ orbitals with a high contribution from carbon $2p_x$ and $2p_y$ orbitals (26%). The computed charge on the carbon atom rises from −0.05 to −1.09 as a consequence. Interestingly the metal–carbon overlap populations remain essentially unchanged (see Table II), confirming the nonbonding nature of these orbitals. Since the model compounds have hydrogen rather than carbonyl ligands, the actual crossover might not occur precisely between $[Co_8(CO)_{18}C]^{2-}$ and $[Ni_8(CO)_{16}C]^{2-}$, but the general point remains that if the cavity size is increased there will at some point be an abrupt change in the charge on the carbon atom, which should be reflected in a greater reactivity toward electrophiles.[11]

This cavity effect has been underlined by calculations on square-antiprismatic and bicapped square-antiprismatic clusters with larger second-row atoms that match the cavity size more effectively, i.e., examples **9** and **10** in Table II. The calculated charges on the interstitial P and Si atoms return to being close to electroneutrality, i.e., 0.00 and 0.31 for phosphorus and silicon atoms, respectively. Cluster compounds having these encapsulated main group atoms have been characterized.[16]

The location of the carbon atom at the center of the cluster even when the cluster cavity volume is large is energetically favorable within the approximations of the extended Hückel method. Calculations on the model bicapped square-antiprismatic cluster (**7**) have shown that the computed total energy rises by 4.0 eV when the carbon atom is displaced by 1.06 Å from the center,

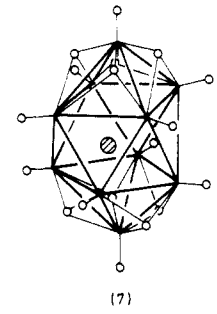

(7)

i.e., to the center of one of the squares of metal atoms. This results partly from a loss of radial bonding between the metal atoms and carbon and increased antibonding interactions between the carbon 2p orbitals and filled d ($D^{\pi}_{\pm 1}$, $F^{\pi}_{\pm 1}$) orbitals on the metal cluster with matching symmetry characteristics. This is shown below, in **13**, for the $L^{\sigma/\pi}_{1c}$ components. The appearance of the destabilizing interaction between the occupied $D^{\pi}_{\pm 1}$ metallic levels and the carbon 2p orbitals is due to the lowering of symmetry of **7** from D_{4d} to C_{4v} when the carbido atom is displaced. For an icosahedral cluster the potential energy surface for the displacement of the carbon atom is much softer (0.4 eV for a 0.6-Å displacement toward the apical metal atom), but the symmetrical location is still favored.

Stabilization of C–H Fragments?

Although the previous calculations indicate that the carbon atom is unlikely to move away from the centroid of the cluster spontaneously, this displacement could become energetically favorable

(14) These asymmetric charge effects may be reflected in the chemical shift tensors in ^{13}C NMR (Heaton, B. T., personal communication).

(15) $[Co_8(CO)_{18}C]^{2-}$ can undergo consecutive reversible one-electron reductions: Rimmelin, J.; Lemoine, P.; Gross, M.; Mathieu, R.; De Montauzon, D. *J. Organomet. Chem.* **1986**, *309*, 355.

(16) (a) Vidal, J. L.; Walker, W. E.; Pruett, R. L.; Schoening, R. C. *Inorg. Chem.* **1979**, *18*, 129. (b) Vidal, J. L.; Walker, W. E.; Schoening, R. C. *Inorg. Chem.* **1981**, *20*, 238. (c) Vidal, J. L. *Inorg. Chem.* **1981**, *20*, 243. (d) Ciani, G.; Garlaschelli, L.; Sironi, A.; Martinengo, S. *J. Chem. Soc., Chem. Commun.* **1981**, 536. (e) Vidal, J. L.; Troup, J. M. *J. Organomet. Chem.* **1981**, *213*, 351. (f) Mackay, K. M.; Nicholson, B. K.; Sims, A. W. *J. Chem. Soc. Chem. Commun.* **1984**, 1276.

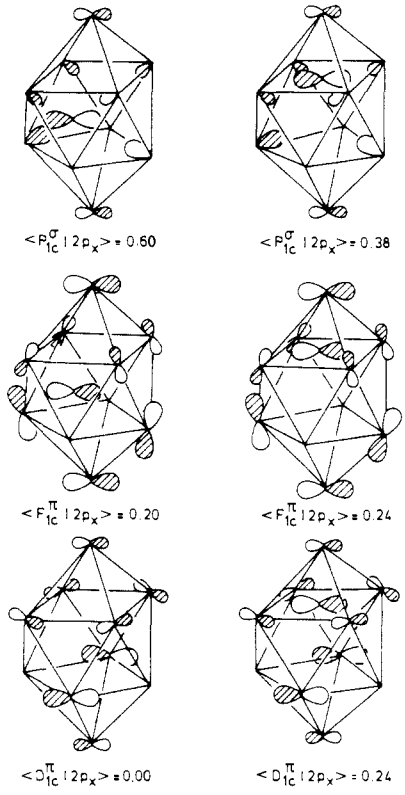

(13)

if a proton enters into the central cavity. When a C–H fragment was located at the center of the bicapped square antiprism (d_{C-H} = 1.00 Å) the metal–hydrogen and metal–carbon lengths have acceptable values, i.e., 1.88 Å to the equatorial atoms. The computed overlap populations are $Co_{equatorial}$–C 0.39, Co_{axial}–C 0.01, and C–H 0.73, cf. 0.79 for ethane. The metal–hydrogen overlap populations are close to zero, however. $[Os_{10}(CO)_{24}(\mu_6\text{-}C)(\mu_4\text{-}H)]^-$ provides an example of a cluster with interstitial carbon and hydrogen atoms in adjacent octahedral and tetrahedral sites (d_{C-H} ca. 1.75 Å),[17] but there are no examples of interstitial C–H units in larger cavities currently.

Conclusion

To date cluster chemists have attempted to enhance the reactivities of carbido ligands by emulating exposed surface sites, e.g., the butterfly $[Fe_4(CO)_{12}C]^{2-}$ cluster. These theoretical calculations suggest a completely new mode for activating carbido ligands. Their location in large cavities can lead to a sudden and substantial buildup of negative charge if the low-lying M–C nonbonding $L^{\sigma/\pi}$ orbitals with a high proportion of carbon 2p character enter into the skeletal bonding region. Besides making the carbon atom more reactive to electrophilic reagents the large cavity affords the possibility of stabilizing intermediate species such as C–H.

Reports that square-antiprismatic carbido clusters react with strong protonic acids to give hydrocarbons much more readily than octahedral clusters provide some encouragement for these proposals.[11]

Table III. Extended Hückel Parameters

orbital		H_{ii}, eV	exponents ζ_1	ζ_2
H	1s	−13.60	1.3	
C	2s	−21.40	1.625	
	2p	−11.40	1.625	
O	2s	−32.30	2.275	
	2p	−14.80	2.275	
Si	3s	−17.30	1.383	
	3p	−9.20	1.383	
P	3s	−18.60	1.75	
	3p	−14.00	1.30	
Co	4s	−9.21	2.00	
	4p	−5.29	2.00	
	3d	−13.18	5.55 (0.568)	2.10 (0.606)

Appendix

The calculations were performed within the Extended Hückel method.[18] The atomic parameters are listed in Table III. The carbonyl ligands were modeled by H^- (L in text). Similar results obtained for $[Co_5(CO)_{15}C]^{2+}$ (**2**) and $[Co_5L_{15}C]^{2-}$ (**2′**) support such an approximation (see Table II). In all the idealized geometry models the following bond distances (Å) were used: Co–Co = 2.54, Co–C(O) = 1.80, C–O = 1.15, Co–H = 1.70. Unless otherwise specified, the carbido atom was placed at the center of the polyhedra.

Acknowledgment. The S.E.R.C. is thanked for financial support. The permanent address of J.-F. Halet is at the Laboratoire de Cristallochimie, U.A. 254, of the University of Rennes, France, and his stay at Oxford was made possible by a grant from an Exchange Program between the Royal Society and the C.N.R.S.

Registry No. 1, 111268-04-3; **2**, 111291-01-1; **2′**, 111268-05-4; **3**, 111268-06-5; **4**, 111268-07-6; **5**, 111291-02-2; **6**, 111291-03-3; **7**, 111291-04-4; **8**, 111268-08-7; **9**, 111323-44-5; **10**, 111268-09-8.

(17) Jackson, P. F.; Johnson, B. F. G.; Lewis, J.; McPartlin, M.; Nelson, W. J. H. *J. Chem. Soc., Chem. Commun.* **1982**, 48.

(18) (a) Hoffmann, R. *J. Chem. Phys.* **1963**, *39*, 1397. (b) Hoffmann, R.; Lipscomb, W. N. *Ibid.* **1962**, *36*, 2179, 3189; *37*, 2872.